Mechanism of different switching directions in graphene oxide based RRAM

Wang, Zhongrui; Tjoa, Verawati; Wu, L.; Liu, W. J.; Fang, Z.; Tran, Xuan Anh; Wei, J.; Zhu, W. G.; Yu, Hongyu

2012

Wang, Z., Tjoa, V., Wu, L., Liu, W. J., Fang, Z., Tran, X. A., et al. (2012). Mechanism of different switching directions in graphene oxide based RRAM. Journal of the electrochemical society, 159(6), K177-K182.

https://hdl.handle.net/10356/96219

https://doi.org/10.1149/2.068206jes

Journal of The Electrochemical Society, **159** (6) K177-K182 (2012)
0013-4651/2012/159(6)/K177/6/$28.00 © The Electrochemical Society

Mechanism of Different Switching Directions in Graphene Oxide Based RRAM

Zhongrui Wang,[a] V. Tjoa,[b] L. Wu,[a] W. J. Liu,[a,c] Z. Fang,[a] X. A. Tran,[a] J. Wei,[b] W. G. Zhu,[a] and H. Y. Yu[d,z]

[a]*School of Electrical and Electronic Engineering, Nanyang Technological University, Singapore 639798*
[b]*Singapore Institute of Manufacturing Technology, A*STAR, Singapore 638075*
[c]*School of Electronics Information Engineering, Tianjin Key Laboratory of Film Electronic and Communication Devices, Tianjin University of Technology, Tianjin 300384, China*
[d]*South University of Science and Technology of China, Guangdong 518055, China*

Resistive switching in Graphene Oxide (GO) based RRAM has been studied in combination with various commonly used electrodes e.g. Al, Cu, Ni and Ti. For the first time, coexistence of different reproducible switching directions has been observed in the Al/GO/Pt and the Ti/GO/Pt RRAM cells. These switching directions are correlated to the underlying switching mechanisms as revealed by field dependence, temperature dependence and area dependence. Our observation also suggests that both oxygen related functional groups absorption/release and electrode metal ions diffusion play important roles in bipolar resistive switching of GO.
 [DOI: 10.1149/2.068206jes]

Manuscript submitted December 15, 2011; revised manuscript received March 12, 2012. Published April 5, 2012.

A large variety of materials have been reported with resistive switching characteristics, such as metal oxide,[1,2] perovskite,[3] metal sulfide,[4] metal nitride[5] and carbon based materials.[6] In particular, Graphene Oxide (GO) has been recently explored for RRAM application due to the ease of preparation, potential application to flexible non-volatile memory and all carbon electronics.

The resistive switching in GO was first observed by He et al. in Cu/GO/Pt structure in 2009,[6] which was soon confirmed by Hong et al. on Al/GO/ITO.[7–9] Studies with different electrodes (i.e. Ag, Au and Ti) and GO recipes (i.e. reduced GO) were reported subsequently.[10–16] The underlying switching mechanisms in GO was under debate. (See Table I) For bipolar switching, two interpretations had been proposed. The first suggested that the absorption and release of oxygen related functional groups were responsible for the bipolar switching in GO, which shared resemblance with homogeneous Valence Change Mechanism (VCM) type switching in inorganic materials.[17] This explanation received partial support from REBIC profile at the GO/metal interface and XPS depths profile of oxygen where High Resistance State (HRS) and Low Resistance State (LRS) were identified with distinct oxygen bonding near the interface.[10,14,18] Besides, as the switching was homogeneous, it should be accompanied with strong area dependence, which had been witnessed by Hong et al. [18] The other interpretation of bipolar switching in GO was based on the diffusion of metallic ions from the electrodes, which was similar to the Electrochemical Metallization mechanism (ECM). This was partially supported by the observed Ohmic transport.[6–9,12,16,18] (i.e. linear field dependence in LRS and temperature independent R_{LRS}. See Table I also.) And a recent XPS study on Al/GO/ITO had also suggested the possibility of Al diffusion in GO.[18] Unipolar resistive switching in reduced GO was first reported by Vasu et al. in Al/RGO/ITO where the switching had been attributed to Nanoelectromechanical (NEM) effect.[15] Besides, for bipolar switching in GO, different switching directions had been observed.(See Table II) The origin of these switching directions and their implication to switching mechanism are of great importance to understand the underlying mechanism.

In this work, coexistence of different switching directions in GO based RRAM was observed by investigating Metal/GO/Pt structures with different active metal electrodes. Transport measurement (i.e. field dependence, temperature dependence and area dependence) revealed these switching directions were underlying mechanisms oriented. And both absorption/release of oxygen related functional groups and diffusion of metal electrode ions were identified of important roles in bipolar switching of GO.

[z]E-mail: yu.hy@sustc.edu.cn

Experimental

In GO RRAM devices (Fig. 1a), Pt electrode of ∼40 nm was deposited by electron beam evaporation on Si substrate with a Ti adhesion layer. The GO solution was prepared by oxidation of graphite powder using modified Hummer's and Offeman's method. Briefly, graphite powder, Sodium Nitrate and Sulfuric acid were mixed and stirred for 10 minutes. Then, Potassium Permanganate was added while solution was put in ice bath. DI water was added while temperature was raised to 90°C. After an hour, Hydrogen peroxide was added drop wise and the solution turned yellow. The mixture was filtered while warm and washed with warm DI water. Purification was done by centrifugation to remove un-oxidized particle and graphene oxide flakes. A 60 nm thick GO thin film was deposited by drop-casting method, where the SEM images were shown in Fig. 1b and 1c. Four different electrodes, Al, Cu, Ni and Ti were deposited by electron beam evaporation with shadow mask patterning respectively. The top electrode had a thickness of 50 nm and a diameter of 300 μm unless specified otherwise. (See Fig. 1a) Electrical characterization was performed by using a Keithley 4200 semiconductor parameter analyzer and a SUSS probe station.

Results and Discussion

XPS examination of GO film.— The GO film was examined by XPS, as shown in Fig. 1d. As a heavily oxidized graphene oxide film, there were 3 main peaks from C 1s, denoted as Peak 1 (*sp*2 carbon), Peak 2 [epoxy (C–E) group and hydroxyl group (C–OH)] and Peak 3 [ketones (C=O) or edge groups like carboxyl (COOH)], consistent with the literature report.[19]

I–V characteristics and cycle-to-cycle distribution of switching parameters.— The typical anticlockwise (AW) bipolar resistive switching of GO RRAM with different electrode materials was compared in Fig. 3a, 3c, 3d, and 3e with compliance current $I_C = 1$ mA. No switching was found in Ni/GO/Pt RRAM cell, which might be due to the reason that Ni^{2+} could react with hydroxyl group of GO to form conductive $Ni(OH)_2$.[20,21] This might hinder negative voltage sweep from drifting back Ni^{2+} ions. Also, for the absorption of oxygen related functional groups at the Ni/GO interface, the barriers might loss insulating capability due to the formation of $Ni(OH)_2$.[22] For Al/GO/Pt structure and Ti/GO/Pt structure, more than one switching directions were observed (See Fig. 2b and 2f). For Al/GO/Pt, with a 10 μA compliance current, positive voltage sweep brought the as-deposited Al/GO/Pt RRAM cell to the unipolar LRS, which had an I–V curve coinciding with that of bipolar HRS shown in

Table I. Literature summary of mechanisms study on GO based resistive switching.

	Bipolar Switching				Unipolar Switching Nanoelectromechanical Effect (NEM)	
	Oxygen related functional group absorption/ release at the interface		Metal electrode ions diffusion			
Physical Characterization	XPS on Al/GO/Al[10] REBIC on Al/GO/Al[14] XPS on Al/GO/ITO[18]		XPS on Al/GO/ITO[18]		AFM on Al/RGO/ITO[15]	
Field Dependence	Non-linear LRS and HRS field dependence	Al/GO/Al[10]	Linear LRS and non-linear HRS field dependence	Cu/GO/Pt[6] Al/GO/ITO[7–9,18] (Ag,Au,Cu,Ti)/ GO/Pt[12] Al/GO/ITO[16]	Linear LRS and non-linear HRS field dependence	Al/RGO/ITO[15]
Temperature Dependence	N. A.		Temperature Independent R_{LRS} in Cu/GO/Pt[12]		N. A.	
Area Dependence	Area Dependent R_{HRS}, R_{LRS}[18]		N. A.		N. A.	

Fig. 2a and 2b. The V_{RESET} in unipolar switching was ∼1.8 V, relatively higher than the V_{SET} in bipolar switching. As a consequence, unipolar switching might easily trigger a second time breakdown in RESET process and transform to bipolar AW switching. But no reversed transition was observed. This was probably because the bipolar V_{SET} was lower than the unipolar V_{RESET}, which made bipolar AW switching preferable. The endurance of unipolar switching was typically several tens of cycles. For Ti/GO/Pt structure, clockwise (CW) forming free, self-compliance bipolar switching direction was found. (See Fig. 2f) LRS (CW) I–V coincided with HRS (AW) I–V (See Fig. 2e and 2f) too. Since RESET process was of a high voltage ∼2 V, it might cause a subsequent breakdown. Thus, the device would eventually move to bipolar AW switching after tens of cycles. Also, no reversed transition was found because bipolar AW V_{SET} (∼1.1 V) was smaller than the maximum sweep voltage (2V). Similar behaviors in $Pt/TiO_2/Pt$ RRAM were reported.[13] The Cu/GO/Pt structure exhibited only single switching direction, which might be caused by huge Cu^{2+} absorption capacity of GO.[23] And diffusion of electrode ions might dominate the switching in the Cu/GO/Pt structure.

Fig. 3 showed the cumulative probability of R_{HRS}, R_{LRS}, V_{SET}, and V_{RESET} distribution of Al, Cu and Ti electrode RRAM structures. Bipolar (AW) resistance magnitude and On/Off ratio of Cu and Ti top electrode RRAM was consistent with reported value.[12] As mentioned, unipolar LRS resistance of Al/GO/Pt was almost the same as that of bipolar HRS due to similar transport natures. (See Fig. 3a) And LRS (CW) state resistance of Ti/GO/Pt coincided with HRS (AW) resistance also. (See Fig. 3e)

Electric field dependence of current.— Fig. 4a showed that LRS (AW) was of an Ohmic behavior with a slope ∼1 in log-log I–V plot consistent with literature report.[6–9,12,16,18] (See Table I also) HRS (AW) showed non-linear field dependence especially in high field region which was of a slope >1.8. This could be explained by space charge limited current where $I \sim aV + bV^2$.[16] On the contrary, as shown in Fig. 4b, bipolar CW switching in Ti/GO/Pt and unipolar switching in Al/GO/Pt had non-Ohmic LRS with slope >1.5 in high field region. Therefore, conduction mechanisms of different directions might be different. In conclusion, bipolar AW switching was observed with linear field dependence in LRS, which suggested Ohmic transport. But unipolar switching in Al/GO/Pt and bipolar CW switching in Ti/GO/Pt were of non-linear field dependence, which might originate from space charge limited current.

Table II. Literature summary of reported bipolar resistive switching direction in GO. Bottom electrode is presumed to be grounded.

Switching Direction	Bipolar Switching		Unipolar Switching
	Clockwise (CW)	Anticlockwise (AW)	
	Al/GO/ITO[7–9,18]	Cu/GO/Pt[6] (Ag, Au, Cu, Ti)/GO/Pt[12] Ag/PI/GO:PI/PI/ITO[11] Al/GO/ITO[16]	Al/RGO/ITO[15]

Temperature dependence of resistance and the instability.— Fig. 5 showed the Arrhenius plot of resistance in Al/GO/Pt, Cu/GO/Pt and Ti/GO/Pt. Distinct R_{LRS} activation energy was observed. For LRS (AW), the E_A was almost zero, which might suggest Ohmic transport again. For HRS (AW), the E_A was ∼46 meV/∼78 meV/∼0.21 eV in Al/Cu/Ti topped GO RRAM cell, respectively, consistent with literature report, which suggested that the transport was thermally activated.[12,13,24]

In Fig. 6a and 6b, temperature instability of switching parameters in the Al/GO/Pt and the Ti/GO/Pt RRAM cells were compared. The fluctuation of resistance and operation voltage during cycling was more severe in high temperature range. For Al/GO/Pt sample, bipolar AW R_{HRS} (similar to unipolar R_{LRS}) was subjected to larger temperature instability while R_{LRS} was more regulated by current compliance. On the contrary, for Ti/GO/Pt RRAM cell, bipolar AW R_{HRS} (similar to bipolar CW R_{LRS}) had much less temperature based fluctuation. (See Fig. 6a). This clued that unipolar switching in Al/GO/Pt was of different mechanism with bipolar CW switching in Ti/GO/Pt.

As a summary, bipolar AW switching was observed with temperature insensitive R_{LRS}, which again suggested Ohmic transport. On the contrary, the R_{LRS} of the unipolar switching Al/GO/Pt and the bipolar CW switching Ti/GO/Pt were of much larger activation energy, which suggested thermal facilitated transport.

Area dependence of resistance.— As shown in Fig. 7, the bipolar AW switching and the unipolar switching were observed of weakly area dependent R_{LRS}, this suggested a filament type transport. However, R_{LRS} of bipolar CW switching in Ti/GO/Pt showed strong area dependence, which was consistent with the oxygen related functional groups release/absorption model.[18]

Retention and endurance.— Fig. 8a was a retention test at room temperature on Ti/GO/Pt structure. Both AW and CW directions were tested, which showed no clear degradation in 10^3 seconds. Similar retention characteristic was found for Al/GO/Pt. Fig. 8b was the DC cycling endurance of bipolar AW switching Ti/GO/Pt. The performance could retain up to 500 cycles.

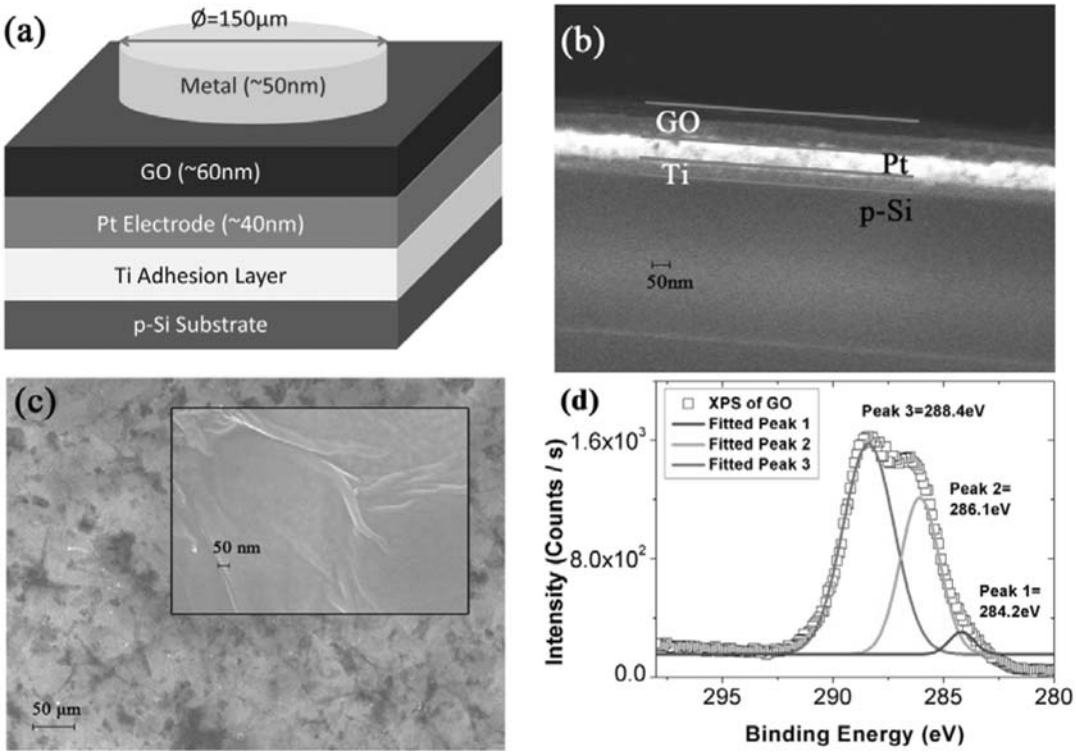

Figure 1. (a) Sketch of Metal/GO/Pt sandwiched structure. (b) (c) SEM cross section and top view images of GO film on Pt substrate. Inset of (c) shows the image of a single GO flake. (d) XPS spectrum of C 1s. Main peaks P1, P2 and P3 are at 284.2 eV, 286.1 eV and 288.4 eV, respectively, in consistent with literature report.

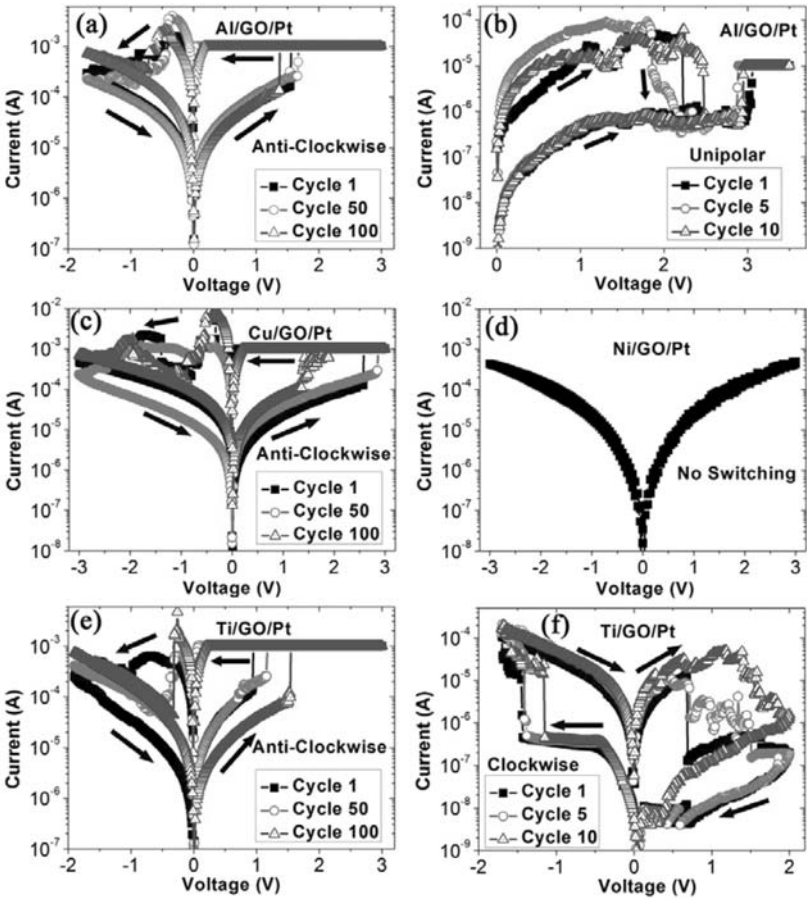

Figure 2. (a) (c) (e) Typical bipolar AW switching I–V curves of GO with Al, Cu, Ti top electrodes (I_C = 1 mA). (b) Unipolar switching I–V curves in Al/GO/Pt (I_C = 10 μA). (d) No switching in Ni/GO/Pt. (f) Bipolar CW switching I–V curves in Ti/GO/Pt.

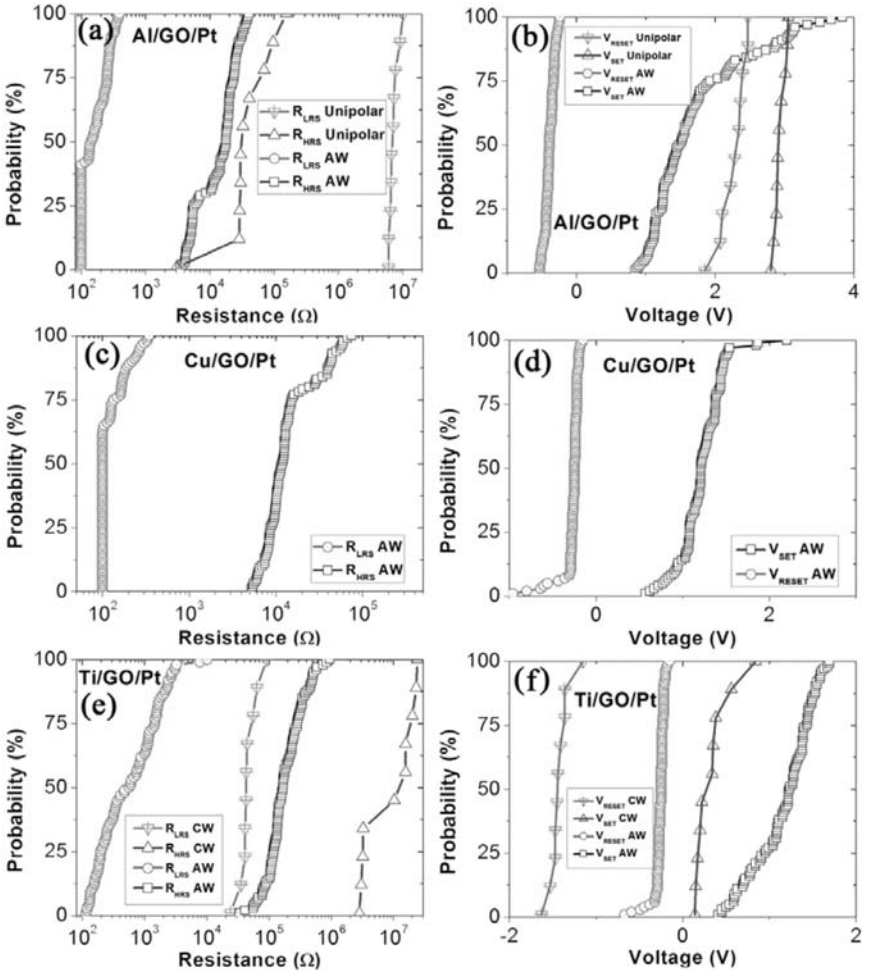

Figure 3. Cumulative probability of bipolar switching (AW/CW) and unipolar switching R_{HRS} (measured at −0.1 V) and R_{LRS} (measured at 0.1 V) in (a) Al/GO/Pt, (c) Cu/GO/Pt, (e) Ti/GO/Pt. $I_C = 1$ mA in positive voltage range. Cumulative probability of bipolar switching (AW/CW) and unipolar switching V_{SET} (defined as the point with maximum slope change) and V_{RESET} (defined as the point with maximum slope change) in (b) Al/GO/Pt, (d) Cu/GO/Pt, (f) Ti/GO/Pt. $I_C = 1$ mA in positive voltage range.

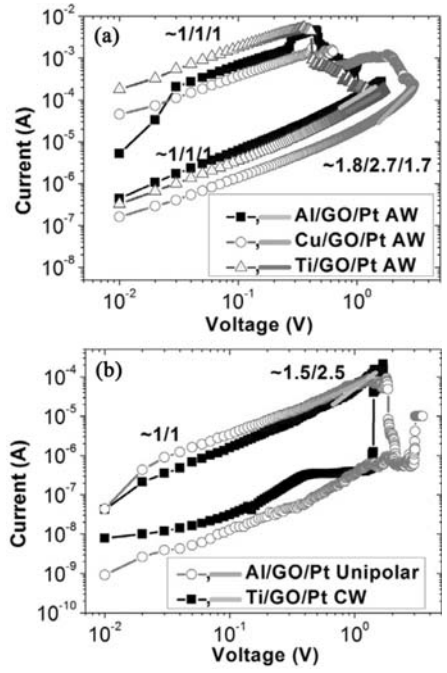

Figure 4. (a) Field dependence of bipolar AW switching I–V in Al/GO/Pt, Cu/GO/Pt and Ti/GO/Pt. All LRS (AW) are of slope ∼1. (b) Field dependence of unipolar switching in Al/GO/Pt and CW bipolar switching in Ti/GO/Pt. All LRS (Unipolar or CW) are of slope >1 in the high field region.

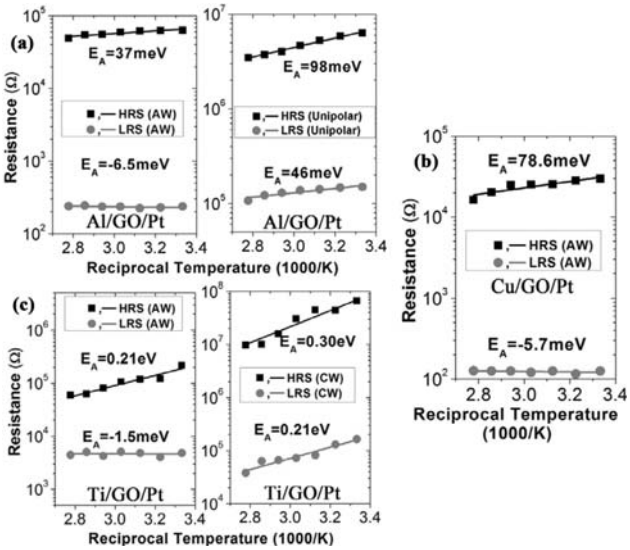

Figure 5. (a) (b) (c) Arrhenius plot of R_{HRS} and R_{LRS} in Al/GO/Pt, Cu/GO/Pt and Ti/GO/Pt under different switching directions, respectively.

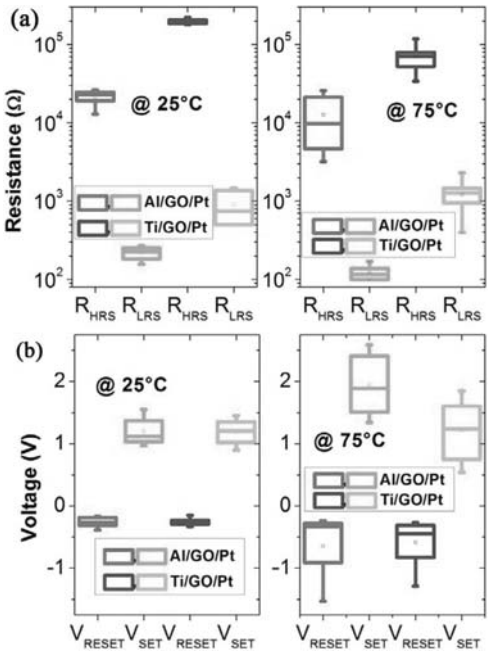

Figure 6. (a) Distribution of R_{HRS} and R_{LRS} in Al/GO/Pt and Ti/GO/Pt structure at 25°C and 75°C (b) Distribution of V_{SET} and V_{RESET} in Al/GO/Pt and Ti/GO/Pt structure at 25°C and 75°C.

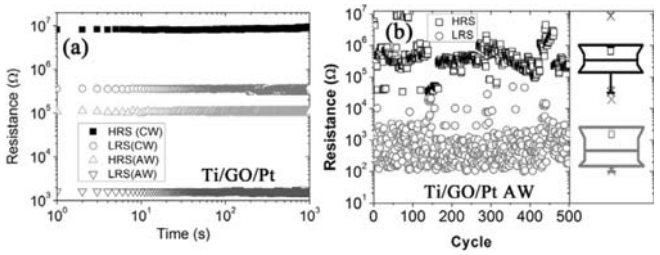

Figure 8. (a) Room temperature retention of Ti/GO/Pt. (b) Room temperature D. C. endurance of bipolar AW switching Ti/GO/Pt.

Conclusions

Resistive switching in GO based RRAM had been studied with Al, Cu, Ni and Ti top electrodes. Different reproducible switching directions had been found in the Al/GO/Pt and the Ti/GO/Pt RRAM. Through analysis of the field dependence, the temperature dependence and the area dependence, the conduction mechanisms were found to be different in these directions, which were summarized in Table III. The transport measurement indicated switching direction was underlying mechanism oriented. (See Table III also) The bipolar AW switching might associate with the diffusion of metal electrode ions while the bipolar CW switching was due to the absorption/release of oxygen based functional groups, consistent with literature.[12,18] The unipolar switching in Al/GO/Pt might be caused by NEM effect, as reported in literature.[15] And the coexistence of two bipolar switching directions in Ti/GO/Pt also showed that both the oxygen related functional group absorption/release and the electrode metal ions diffusion play important role in the resistive switching of GO.

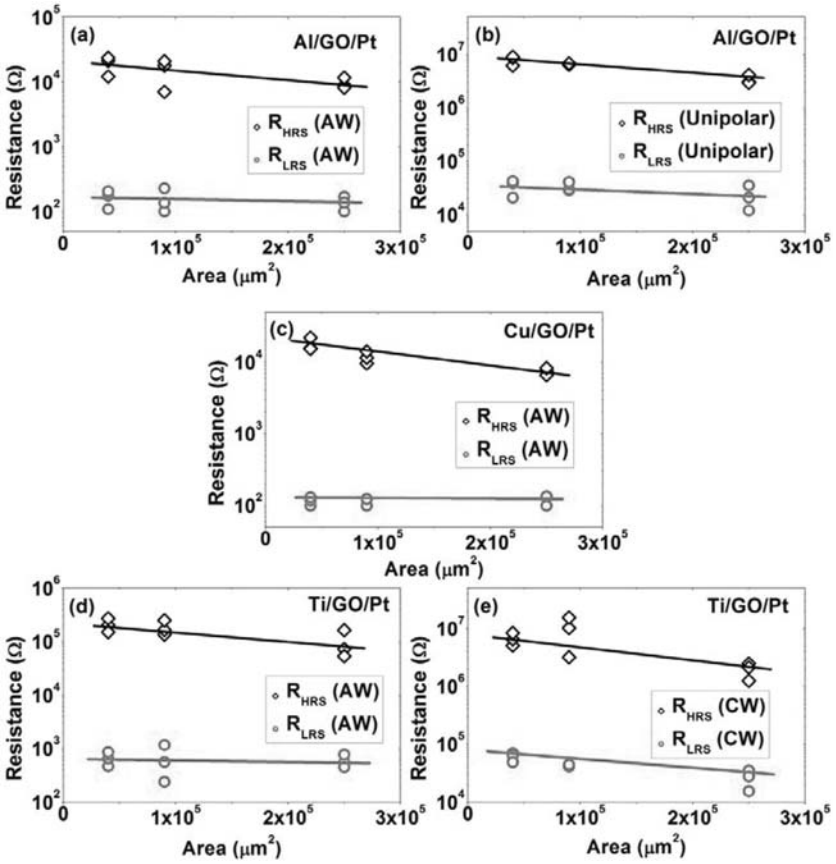

Figure 7. Area dependence of R_{HRS} and R_{LRS} in (a) Bipolar AW switching Al/GO/Pt RRAM cell (b) Unipolar switching Al/GO/Pt RRAM cell (c) Bipolar AW switching Cu/GO/Pt RRAM cell (d) Bipolar AW switching Ti/GO/Pt RRAM cell (e) Bipolar CW switching Ti/GO/Pt RRAM cell.

Table III. Summary of the observed transport characteristics.

		AW			Unipolar or CW	
		Al/GO/Pt	Cu/GO/Pt	Ti/GO/Pt	Al/GO/Pt	Ti/GO/Pt
Field Dependence	HRS	Non-linear	Non-linear	Non-linear	Non-linear	Non-linear
	LRS	***Linear***	***Linear***	***Linear***	***Non-linear***	***Non-linear***
Temperature Dependence	HRS	Strong	Strong	Strong	Strong	Strong
	LRS	***Weak***	***Weak***	***Weak***	***Strong***	***Strong***
Area Dependence	HRS	Strong	Strong	Strong	Strong	Strong
	LRS	***Weak***	***Weak***	***Weak***	***Weak***	***Strong***
Suggested Mechanism		Electrode metal ions migration			NEM	O-group absorption/release

References

1. H. Y. Lee, et al., in *IEDM Tech. Dig.* (2008), p. 1.
2. H. Akinaga and H. Shima, *Proc. IEEE*, **98**, 2237 (2010).
3. L. Chun-Chieh, T. Bing-Chung, L. Chao-Cheng, L. Chen-Hsi, and T. Tseung-Yuen, *IEEE Electron Device Lett.*, **27**, 725 (2006).
4. T. Sakamoto, H. Sunamura, H. Kawaura, T. Hasegawa, T. Nakayama, and M. Aono, *Appl. Phys. Lett.*, **82**, 3032 (2003).
5. C. Chen, Y. C. Yang, F. Zeng, and F. Pan, *Appl. Phys. Lett.*, **97**, 083502 (2010).
6. C. L. He, et al., *Appl. Phys. Lett.*, **95**, 232101 (2009).
7. H. Seul Ki, K. Ji Eun, K. Sang Ouk, C. Sung-Yool, and C. Byung Jin, *IEEE Electron Device Lett.*, **31**, 1005 (2010).
8. S. K. Hong, J.-E. Kim, S. O. Kim, and B. J. Cho, in *2010 10th IEEE Conference on Nanotechnology, NANO 2010, August 17, 2010–August 20, 2010* (2010), p. 604.
9. H. Seul Ki and C. Byung Jin, in *Nanoelectronics Conference (INEC), 2011 IEEE 4th International* (2011), p. 1.
10. H. Y. Jeong, et al., *Nano Lett.*, **10**, 4381 (2010).
11. C. Wu, F. Li, Y. Zhang, T. Guo, and T. Chen, *Appl. Phys. Lett.*, **99**, 042108 (2011).
12. F. Zhuge, B. Hu, C. He, X. Zhou, Z. Liu, and R.-W. Li, *Carbon*, **49**, 3796 (2011).
13. O. O. Ekiz, M. Urel, H. Guner, A. K. Mizrak, and A. Dana, *ACS Nano*, **5**, 2475 (2011).
14. G. N. Panin, O. O. Kapitanova, S. W. Lee, A. N. Baranov, and T. W. Kang, *Japanese Journal of Applied Physics*, **50**, 070110 (2011).
15. K. S. Vasu, S. Sampath, and A. K. Sood, *Solid State Commun.*, **151**, 1084 (2011).
16. L.-H. Wang, W. Yang, Q.-Q. Sun, P. Zhou, H.-L. Lu, S.-J. Ding, and D. Wei Zhang, *Appl. Phys. Lett.*, **100**, 063509 (2012).
17. R. Waser, R. Dittmann, G. Staikov, and K. Szot, *Adv. Mater.*, **21**, 2632 (2009).
18. S. K. Hong, J. E. Kim, S. O. Kim, and B. J. Cho, *J. Appl. Phys.*, **110** (2011).
19. W. Zhang, V. Carravetta, Z. Li, Y. Luo, and J. Yang, *The Journal of Chemical Physics*, **131**, 244505 (2009).
20. H. Wang, H. S. Casalongue, Y. Liang, and H. Dai, *J. Am. Chem. Soc.*, **132**, 7472 (2010).
21. B. Li, H. Cao, J. Shao, H. Zheng, Y. Lu, J. Yin, and M. Qu, *Chem. Commun.*, **47**, 3159 (2011).
22. M.-S. Wu, Y.-P. Lin, C.-H. Lin, and J.-T. Lee, *J. Mater. Chem.*, **22**, 2442 (2012).
23. S. T. Yang, Y. Chang, H. Wang, G. Liu, S. Chen, Y. Wang, Y. Liu, and A. Cao, *J. Colloid Interface Sci.*, **351**, 122 (2010).
24. A. Yildiz, F. Iacomi, and D. Mardare, *J. Appl. Phys.*, **108**, 083701 (2010).